The Astrophysical Journal, 667: L141–L144, 2007 October 1

ON THE METALLICITY DEPENDENCE OF THE 24 μm LUMINOSITY AS A STAR FORMATION TRACER

M. Relaño,[1] U. Lisenfeld,[1] P. G. Pérez-González,[2,3] J. M. Vílchez,[4] and E. Battaner[1]

Received 2007 May 22; accepted 2007 August 13; published 2007 September 18

ABSTRACT

We investigate the use of the rest-frame 24 μm luminosity as an indicator of the star formation rate (SFR) in galaxies with different metallicities by comparing it to the (extinction-corrected) Hα luminosity. We carry out this analysis in two steps: First, we compare the emission from H II regions in different galaxies with metallicities between 12 + log (O/H) = 8.1 and 8.9. We find that the 24 μm and the extinction-corrected Hα luminosities from individual H II regions follow the same correlation for all galaxies, independent of their metallicity. Second, the role of metallicity is explored further for the integrated luminosity in a sample of galaxies with metallicities in the range of 12 + log (O/H) = 7.2–9.1. For this sample we compare the 24 μm and Hα luminosities integrated over the entire galaxies and find a lack of the 24 μm emission for a given Hα luminosity for low-metallicity objects, likely reflecting a low dust content. These results suggest that the 24 μm luminosity is a good metallicity-independent tracer for the SFR in individual H II regions. On the other hand, metallicity has to be taken into account when using the 24 μm luminosity as a tracer for the SFR of entire galaxies.

Subject headings: galaxies: ISM — infrared: galaxies

1. INTRODUCTION

The total infrared (IR) emission is known to be an optimum tracer of the star formation rate (SFR) for highly obscured star-forming regions (Kennicutt 1998; Sanders & Mirabel 1996). Observationally, the power of the IR (especially the mid-IR) to trace star formation (SF) has been confirmed using *Infrared Space Observatory* data (Genzel & Cesarsky 2000). Detailed studies of extended SF along the spiral arms of normal disk galaxies carried out by Roussel et al. (2001) showed that the SFR can be parameterized by the luminosity at 7 or 15 μm, and this has been confirmed by a recent study of 20 spiral and starburst galaxies (Forster Schreiber et al. 2004). Correlations of the total IR luminosity and the luminosity at 6.7, 12, and 15 μm are shown in Chary & Elbaz (2001).

After the launch of the *Spitzer Space Telescope* (Werner et al. 2004), new IR wavelength bands have been proposed to trace the SFR in late-type spiral galaxies. Comparisons of these new bands (24 μm from MIPS, Rieke et al. 2004; 8 μm from IRAC, Fazio et al. 2004) with other typical SFR tracers, such as the Hα emission, have shown very good correlations that hold over more than 2 orders of magnitude in luminosity (Calzetti et al. 2005, hereafter CKB; Pérez-González et al. 2006, hereafter PKG). The correlation found between the 24 μm luminosity and the extinction-corrected Hα luminosity for the central H II emitting knots in M51 was later confirmed for the H II regions in M81. In the latter object, the dispersion was, however, found to be higher, which was explained by the significant amount of nonobscured SF and by the large uncertainties in the attenuation estimations. Recently, Calzetti et al. (2007) carried out a detailed study of the mid-IR emission as a SFR indicator and concluded that the 24 μm emission shows a good, however nonlinear relation with the Paα emission. They have also explored the possible role of the metallicity on this relation.

Other studies have investigated the relation between the 24 μm and the extinction-corrected Hα luminosities in other types of galaxies. Alonso-Herrero et al. (2006) obtained the same good correlation between the 24 μm and the extinction-corrected Paα luminosities of luminous infrared galaxies (LIRGs) and ultraluminous infrared galaxies (ULIRGs), which makes the relation applicable over nearly 5 orders of magnitude in luminosity. Wu et al. (2005) also found a good correlation between the integrated 24 and 8 μm luminosities and the Hα luminosity in a sample of star-forming galaxies, but they obtained a change in the slope for the dwarf galaxies of their sample. Cannon et al. (2005, 2006a, 2006b) studied Hα and *Spitzer* data of the dwarf galaxies IC 2574, NGC 1705, and NGC 6822, respectively. They found values for the 24 μm luminosities of the H II regions 3–5 times lower than expected from the Hα luminosity when applying the relation for M51 of CKB. The aim of this Letter is to investigate the reason of the differences found in the references above, and in particular to study the role played by the metallicity in the 24 μm–Hα relation.

2. GALAXY SAMPLE AND DATA ANALYSIS

Our study is based, apart from data of the literature (see below), on our own analysis of the nearby dwarf galaxies NGC 1569 and NGC 4214, for which *Spitzer* MIPS images at 24 μm are available.

The optical data of the dwarf galaxies NGC 1569 and NGC 4214 were taken from the *HST* data archive. The data analysis for the Hα and Hβ images of NGC 1569 is explained in Relaño et al. (2006); for NGC 4214, we obtained Hα and Hβ images following the procedure explained in MacKenty et al. (2000). The Hα fluxes of the most luminous H II regions in NGC 1569 coincide within 10% with the values given by Waller (1991). For NGC 4214 the differences with respect to the fluxes of MacKenty et al. (2000) are less than 16%. The MIPS 24 μm images of these galaxies were taken from the *Spitzer* data archive and reduced using the MIPS data analysis tool (Gordon et al. 2005). The calibration uncertainties amount to ~4% (Engelbracht et al. 2007).

In order to make the Hα and IR photometric analysis in NGC 1569 and NGC 4214, all images were convolved to the resolution of the MIPS 24 μm image, using the semiempirical PSF for a 75 K blackbody.[5] The Hα and 24 μm images have the same ap-

[1] Departamento de Física Teórica y del Cosmos, Universidad de Granada, Avenida Fuentenueva s/n, 18071 Granada, Spain; mrelano@ugr.es, ute@ugr.es, battaner@ugr.es.

[2] Departamento de Astrofísica y CC. de la Atmósfera, Facultad de CC. Físicas, Universidad Complutense de Madrid, 28040 Madrid, Spain; pgperez@astrax.fis.ucm.es.

[3] Associate Astronomer at Steward Observatory, University of Arizona.

[4] Instituto de Astrofísica de Andalucía, CSIC, Apartado 3004, 18080 Granada, Spain; jvm@iaa.es.

[5] See http://dirty.as.arizona.edu/~kgordon/mips/conv_psfs/conv_psfs.html.

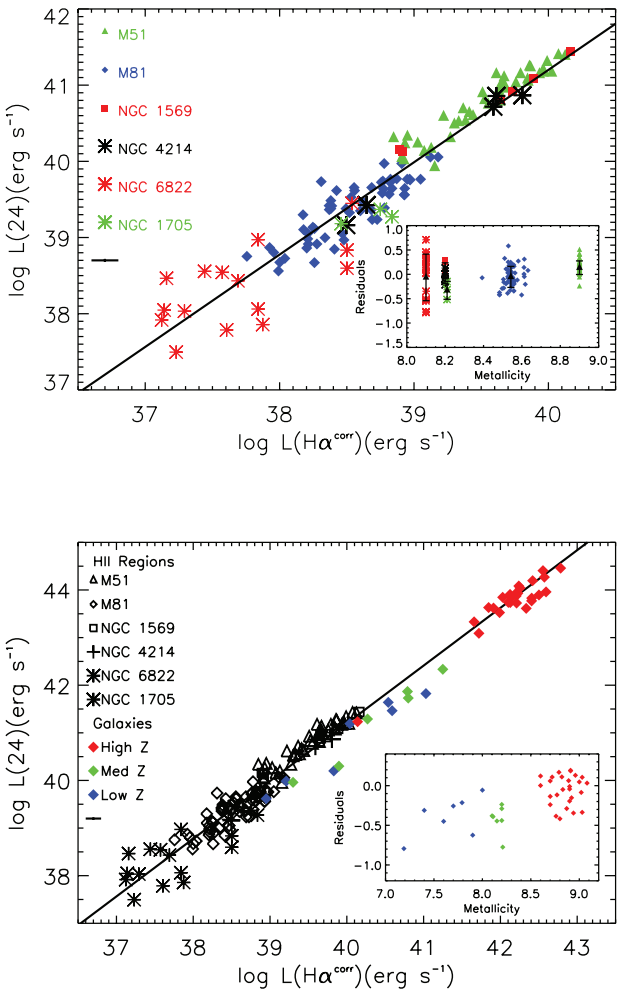

FIG. 1.—*Top*: 24 μm luminosity as a function of the extinction corrected Hα luminosity for a sample of H II regions in M51, M81, NGC 1569, NGC 4214, NGC 6822, and NGC 1705. The solid line shows the linear fit to the H II regions of M51, M81, and the ULIRGs from Alonso-Herrero et al. (2006) (see eq. [1]). Typical error bars are shown in the lower left corner of the plot: they account for uncertainties in the calibration (4% for 24 μm flux (Engelbracht et al. 2007), ~15% for Hα flux, and ~0.2 mag for the extinctions (Gil de Paz et al. 2003; Relaño et al. 2006). In the inner panel we show the residuals of the 24 μm luminosity (see text) vs. the metallicity. The black triangles represent the mean value of the residuals for each galaxy. *Bottom*: The same plot as above but including the integrated luminosities of the galaxies in Table 1. The solid line is the linear fit shown in eq. (1). We use different colors for galaxies with different metallicities: $Z \leq 8.0$ (*blue*), $8.0 < Z < 8.5$ (*green*), and $Z \geq 8.5$ (*red*). In the inner panel we show the residuals of the 24 μm luminosity with respect to linear fit (eq. [1]) vs. the metallicity.

pearance: intense knots observed in Hα match with bright emission at 24 μm. For NGC 1569, we selected six apertures corresponding to the most luminous H II regions catalogued in Waller (1991). In addition, two of these apertures contain a nearby less luminous H II region, which we could not resolve separately due to the coarse spatial resolution (~6″) of our images. In the case of NGC 4214, the apertures selected correspond to the largest H II complexes defined in Table 2 of MacKenty et al. (2000). In both objects, we selected the aperture size (between 11″ and 33″, corresponding to 200–300 pc) individually to match the size of each H II region. Finally, aperture corrections derived from the theoretical PSF at 24 μm were applied to the Hα and 24 μm luminosities.

The Balmer extinction of the H II regions in NGC 1569 was obtained from the corresponding integrated Hα and Hβ fluxes and following Caplan & Deharveng (1986). The extinction values for each H II region agree with those in the extinction map shown in Relaño et al. (2006). Extinction values for each H II region in NGC 4214 were taken from MacKenty et al. (2000), who applied a foreground dust screen model and used bidimensional spectroscopy studies from Maíz-Apellániz et al. (1998).

We also used 24 μm and Hα luminosities integrated over the entire galaxies (see Table 1 for the values and their references). For the Hα luminosity of M51 we applied an extinction correction of $A_{H\alpha} = 1$ mag, which is an intermediate value to those given in CKB for the central part of the galaxy and the values reported in Bresolin et al. (2004) for the H II regions in the outer part of the galaxy. We estimate the uncertainty in the extinction to be ~1 mag, resulting in an uncertainty in the extinction-corrected Hα luminosity of 0.4 dex. For M81, the observed Hα flux was corrected with an extinction of $A_{H\alpha} = 0.3$ mag, derived using an average value of the interstellar reddening map of M81 (Kong et al. 2000) and the extinction law of Draine (2003) with $R_V = 3.1$. From the spatial variations of the reddening map of this galaxy we estimate an uncertainty of 0.3 mag, resulting in an uncertainty of the extinction-corrected Hα luminosity of 0.12 dex. For NGC 1569 we used the mean value of the total extinction given by Devost et al. (1997), $A_{H\alpha} = 1.78$ mag, in agreement with Relaño et al. (2006); and for NGC 4214, $A_{H\alpha} = 0.3$ mag, derived from maps of the Balmer ratio shown in Maíz-Apellániz et al. (1998) and applied by MacKenty et al. (2000). For both galaxies we estimate the uncertainty to be 0.3 mag, yielding in an uncertainty of the extinction-corrected Hα luminosity of 0.12 dex. The Hα luminosities of NGC 1705, NGC 6822, and IC 2574 were not corrected for internal extinction, which was, however, shown to be small (Cannon et al. 2005, 2006a, 2006b).

Finally, we have included a sample of dwarf galaxies covering a wide range of metallicities. The sample is composed of the dwarfs observed by MIPS (Engelbracht et al. 2005), counting with published Galactic extinction-corrected Hα fluxes (Gil de Paz et al. 2003). Given the low metallicity of these dwarf galaxies, internal extinction should be small and is not expected to affect the conclusions of our study. We also added galaxies from the LIRG and ULIRG sample of Alonso-Herrero et al. (2006) with metallicity values available in the literature. We eliminated two galaxies (IC 860 and NGC 7469) of this sample showing high *IRAS* infrared emission from their nucleus, possibly due to an active galactic nucleus. The combined galaxy sample, extinction-corrected (as described above) Hα and 24 μm luminosities, together with the metallicities and distances, are listed in Table 1.

3. RESULTS

In Figure 1 (*top panel*) we compare the extinction-corrected Hα luminosities and the 24 μm luminosities for the H II regions in NGC 1569 and NGC 4214 with those published for M51 (CKB), M81 (PKG), NGC 1705 (Cannon et al. 2006b), and NGC 6822 (Cannon et al. 2006a). The data points of the three low-metallicity galaxies (NGC 1569, NGC 4214, and NGC 6822) follow closely the same distribution as the combined data set of the higher metallicity galaxies M51 and M81 (*triangles and diamonds, respectively*). The H II regions of NGC 6822, representing the lowest luminosities, show a larger scatter than the rest of the H II regions. A possible reason could be the fact that the surface brightness of the H II regions in NGC 6822 is 1–2 orders of magnitude lower than the surface brightness of the H II regions in the other objects. In order to search

TABLE 1
GALAXY SAMPLE AND METALLICITIES

Galaxy	log (L_{24}) (ergs s^{-1})	Reference	log ($L_{H\alpha}^{corr}$) (ergs s^{-1})	Reference	Z	Reference	D (Mpc)
I Zw 18	40.20	1, 2	39.83	8	7.2	11	12.6
HS 0822+3542	39.62	2	38.95	8	7.4	12	10.1
Tol 65	41.46	2	40.59	8	7.6	11	36.0
VII Zw 403	39.99	2	39.21	8	7.7	13	4.8
II Zw 70	41.64	1	40.54	8	7.8	14	18.7
NGC 4861	41.82	2	41.03	8	7.9	15	12.6
Mrk 1450	41.19	2	40.04	8	8.0	16	14.7
I Zw 40	42.33	2	41.25	8	8.1	11	9.8
NGC 6822	39.96	3	39.30	3	8.1	17	0.49
IC 2574	40.73	4	39.98	9	8.15	18	4.0
NGC 1705	40.30	5	39.90	5	8.21	19	5.1
NGC 4670	41.87	2	40.79	8	8.2	20	15.3
NGC 1569	41.73	1	40.80	1	8.2	21	2.2
NGC 4214	41.29	1	40.27	1	8.2	11	2.9
IC 4518A	43.87	6	42.21	6	8.6	22	69.9
IC 4518B	43.33	6	41.66	6	8.6	22	69.9
NGC 5135	43.92	6	42.20	6	8.7	23	52.2
NGC 2537	41.23	2	40.14	8	8.7	24	6.9
M81	41.99	7	40.85	1, 10	8.7	25	3.6
MCG −02-33-098	44.04	6	42.26	6	8.7	26	72.5
NGC 7771	43.96	6	42.59	6	8.8	26	57.1
NGC 3690	44.46	6	42.78	6	8.8	27	47.7
NGC 7130	44.08	6	42.24	6	8.8	26	66.0
UGC 3351	43.61	6	42.34	6	8.8	28	60.9
NGC 3256	44.41	6	42.55	6	8.8	29	35.4
IC 4687	44.27	6	42.57	6	8.8	23	74.1
IC 5179	43.83	6	42.41	6	8.9	26	46.7
M51	43.09	4	41.72	1, 10	8.9	24	8.2
IRAS 17138−1017	44.20	6	42.42	6	8.9	23	75.8
NGC 2369	43.74	6	42.10	6	8.9	26	44.0
NGC 6701	43.74	6	42.13	6	8.9	26	56.6
NGC 633	43.63	6	41.85	6	8.9	23	67.9
NGC 7591	43.85	6	42.03	6	8.9	26	65.5
NGC 5653	43.73	6	42.21	6	8.9	26	54.9
NGC 23	43.77	6	42.40	6	8.9	26	59.6
IC 4734	43.91	6	42.13	6	9.0	22	68.6
NGC 5936	43.85	6	42.14	6	9.0	26	60.8
NGC 5734	43.52	6	41.99	6	9.0	26	59.3
NGC 3110	43.90	6	42.50	6	9.0	26	73.5
ESO 320−G030	43.62	6	41.91	6	9.0	30	37.7
NGC 2388	43.93	6	42.23	6	9.1	26	57.8

NOTES.—Z is the oxygen abundance, 12 + log (O/H). We have checked that the derivation of these values is consistent for this sample.

REFERENCES.—(1) This Letter; (2) Engelbracht et al. 2005; (3) Cannon et al. 2006a; (4) Dale et al. 2005; (5) Cannon et al. 2006b; (6) Alonso-Herrero et al. 2006; (7) PKG; (8) Gil de Paz et al. 2003; (9) Miller & Hodge 1994; (10) Greenawalt et al. 1998; (11) Kobulnicky & Skillman 1996; (12) Kniazev et al. 2000; (13) Izotov et al. 1997; (14) Shi et al. 2005; (15) Kobulnicky et al. 1999; (16) Izotov et al. 1994; (17) Lee et al. 2006; (18) Miller & Hodge 1996; (19) Lee & Skillman 2004; (20) Heckman et al. 1998; (21) Kobulnicky & Skillman 1997; (22) Corbett et al. 2003; (23) Kewley et al. 2001; (24) Guseva et al. 2000; (25) Pilyugin et al. 2004; (26) Veilleux et al. 1995; (27) Armus et al. 1989; (28) Baan et al. 1998; (29) Sekiguchi & Wolstencroft 1993; (30) van den Broek et al. 1991.

for differences as a function of metallicity, we have derived a linear fit including the H II regions of the high-metallicity galaxies (M51 and M81) and the ULIRG sample of Alonso-Herrero et al. (2006), yielding

$$\log L(24) = (-7.28 \pm 0.52) + (1.21 \pm 0.01) \log L(\mathrm{H}\alpha^{\mathrm{corr}}). \quad (1)$$

The slope of this fit is similar to the linear fit obtained by Calzetti et al. (2007) for the high-metallicity data points of their sample, derived using their equations (6) and (9). In the inner plot of Figure 1 (*top panel*) we show the residuals of the 24 μm luminosity (i.e., the difference between the logarithm of the measured 24 μm luminosity and the logarithm of the expected luminosity from the linear fit given in eq. [1]) versus the metallicity of each H II region. For M81 and M51 we estimate the metallicity of the H II regions using the metallicity gradients of each galaxy derived by Pilyugin et al. (2004). For the H II regions in M51 we derive a metallicity variation of <0.1dex for the radial range of their galactocentric radius, and therefore we adopt the central metallicity value for all of them. For the rest of the galaxies in Figure 1 (*top panel*), there is no appreciable metallicity gradients (see references in Table 1). No trend with metallicity is visible, with the mean of the residuals for the H II regions of each galaxy being practically constant over the whole metallicity range. Thus, we conclude that, within the metallicity range investigated here, the relation between the 24 μm and Hα luminosities of H II regions shows no dependence on metallicity.

The situation changes when the integrated galaxy luminosities are considered. In Figure 1 (*bottom panel*) we compare the data for H II regions with the integrated luminosities of the galaxy sample of Table 1, which includes dwarf galaxies with low metallicities and (U)LIRGs with high metallicities. For these additional galaxies, data for individual H II regions are not available. We find a trend that low-metallicity galaxies fall below the linear fit shown in equation (1), whereas the high-metallicity galaxies follow it. In the inner plot of this figure we show again

the residuals of the 24 μm luminosity (with respect to the fit of eq. [1]) versus the metallicity of the galaxy. A trend of lower metallicity galaxies to have a lower ratio of measured-to-expected values is visible, with a correlation coefficient of 0.63. We expect that the uncertainties in the extinction correction of the Hα fluxes will not change this trend for two reasons: The low-metallicity dwarf galaxies, uncorrected for internal extinction, would be located even farther away from the regression fit if we had applied an internal extinction correction, which would further emphasize the observed trend. The rest of the galaxies (except M81 and M51) show only small uncertainties in the adopted extinction values. The higher uncertainties in the case of M81 and M51 are not able to change the general trend observed in the bottom panel of Figure 1.

4. DISCUSSION

It is surprising that the relation between the 24 μm and Hα luminosities for individual H II regions does not show any dependence on metallicities for the range investigated here [galaxies with metallicities between $12 + \log(\mathrm{O/H}) = 8.1$ and 8.9]. A possible reason might be the existence of a lower threshold for the accumulation of dust in H II regions in order to support SFRs as large as the ones measured in our H II regions ($\sim 10^{-4}$ to $10^{-1}\ M_{\odot}\ \mathrm{yr}^{-1}$). This would result in the dust content of H II regions being independent of the global metallicity of the entire galaxy. Support for this hypothesis comes from a detailed study of the Balmer decrement in the major H II regions of NGC 1569 (Relaño et al. 2006), where locally a high intrinsic extinction ($A_V = 0.8$ mag) was found, in spite of the low metallicity of this galaxy. Further studies for higher and lower metallicity galaxies are needed to show how far the universality of the relation between the 24 μm and Hα luminosity extends.

The situation is very different for the ISM outside the H II region, the diffuse ISM, which we take into account when considering the 24 μm and Hα emission integrated over the entire galaxy. Here the 24 μm emission depends directly on the dust content and opacity and hence on the metallicity.

Recently, Calzetti et al. (2007) studied the relation between the 24 μm and the extinction-corrected Paα surface densities of the star forming regions in a sample of nearby galaxies. They found a slight trend for H II regions of low-metallicity galaxies to have a lower 24 μm emission for a given Paα surface density than higher metallicity regions. Their use of a fixed aperture size for the H II regions in all galaxies might have included some diffuse emission, especially for distant galaxies. This would explain the similarity of their results and ours for the integrated emissions. A deeper analysis of the results presented in this letter, including a larger sample of H II regions and separating clearly the diffuse emission from the emission coming from the H II regions is needed (M. Relaño et al. 2007, in preparation).

5. SUMMARY AND CONCLUSIONS

We have studied the role of the metallicity in the use of the 24 μm luminosity as a SFR indicator by analyzing the data for a sample of dwarfs and spirals covering a wide range of metallicities. We found that the extinction-corrected Hα and the 24 μm luminosities correlate tightly for all H II regions, independently of the global metallicity of the galaxy. This demonstrates that the 24 μm luminosity is a good tracer of the *local* SFR, independent of the metallicity. This is not the case when considering the integrated emission of galaxies. In this case, metal-rich galaxies present a higher 24 μm luminosity for a given Hα luminosity than low-metallicity galaxies. Our results indicate that the 24 μm luminosity can be used as a SFR tracer when taking into account (1) whether the emission from H II regions or the integrated emission from entire galaxies is considered and (2) the metallicity of the galaxy.

We would like to thank the anonymous referee and Almudena Zurita for useful suggestions that improved the final version of the manuscript. This work has been supported by the Spanish Ministry of Education and Science within the PNAYA via projects AYA2004-08251-C02-00, and ESP2003-00915. P. G. P.-G. acknowledges support from the Ramón y Cajal Fellowship Program and the project AYA 2006-02358.

REFERENCES

Alonso-Herrero, A., et al. 2006, ApJ, 650, 835
Armus, L., Heckman, T. M., & Miley, G. K. 1989, ApJ, 347, 727
Baan, W., A., Salzer, J. J., LeWinter, R. D. 1998, ApJ, 509, 633
Bresolin, F., Garnett, D. R., & Kennicutt, R. C. Jr. 2004, ApJ, 615, 228
Calzetti, D., et al. 2005, ApJ, 633, 871 (CKB)
———. 2007, preprint (arXiv:0705.3377)
Cannon, J. M., Walter, F., & Armus, L. 2006a, ApJ, 652, 1170
Cannon, J. M., et al. 2005, ApJ, 630, L37
———. 2006b, ApJ, 647, 293
Caplan, J., & Deharveng, L. 1986, A&A, 155, 297
Chary, R., & Elbaz, D. 2001, ApJ, 556, 562
Corbett, E. A., et al. 2003, ApJ, 583, 670
Dale, D. A., et al. 2005, ApJ, 633, 857
Devost, D., Roy, J. R., & Drissen, L. 1997, ApJ, 482, 765
Draine, B. T. 2003, ARA&A, 41, 241
Engelbracht, C. W., et al. 2005, ApJ, 628, L29
———. 2007, preprint (arXiv:0704.2195v1)
Fazio, G. G., et al. 2004, ApJS, 154, 10
Forster Schreiber, N. M., Roussel, H., Sauvage, M., & Charmandaris, V. 2004, A&A, 419, 501
Genzel, R., & Cesarsky, C. J. 2000, ARA&A, 38, 761
Gil de Paz, A., Madore, B. F., & Pevunova, O. 2003, ApJS, 147, 29
Gordon, K. D., et al. 2005, PASP, 117, 503
Greenawalt, B., et al. 1998, ApJ, 506, 135
Guseva, N. G., Izotov, Yu. I., & Thuan, T. X. 2000, ApJ, 531, 776
Heckman, T. M., et al. 1998, ApJ, 503, 646
Izotov, Yu. I., Thuan, T. X., & Lipovetsky, V. A. 1994, ApJ, 435, 647
Izotov, Yu. I., Thuan, T. X., & Lipovetsky, V. A. 1997, ApJS, 108, 1
Kennicutt, R. C. Jr. 1998, ARA&A, 36, 189
Kewley, L. J., Heisler, C. A., Dopita, M. A., & Lumsden, S. 2001, ApJS, 132, 37
Kniazev, A. Yu., et al. 2000, A&A, 357, 101
Kobulnicky, H. A., Kennicutt, R. C. Jr., & Pizagno, J. L. 1999, ApJ, 514, 544
Kobulnicky, H. A., & Skillman, E. D. 1996, ApJ, 471, 211
———. 1997, ApJ, 489, 636
Kong, X., et al. 2000, AJ, 119, 2745
Lee, H., & Skillman, E. D. 2004, ApJ, 614, 698
Lee, H., Skillman, E. D., & Venn, K. 2006, ApJ, 642, 813
MacKenty, J. W., et al. 2000, AJ, 120, 3007
Maíz-Apellániz, J., et al. 1998, A&A, 329, 409
Miller, B. W., & Hodge, P. 1994, ApJ, 427, 656
———. 1996, ApJ, 458, 467
Pérez-González, P. G., et al. 2006, ApJ, 648, 987 (PKG)
Pilyugin, L. S., Vílchez, J. M., & Contini, T. 2004, A&A, 425, 849
Relaño, M., Lisenfeld, U., Vílchez, J. M., & Battaner, E. 2006, A&A, 452, 413
Rieke, G. H., et al. 2004, ApJS, 154, 25
Roussel, H., Sauvage, M., Vigroux, L., & Bosma, A. 2001, A&A, 372, 427
Sanders, D. B., & Mirabel, I. F. 1996, ARA&A, 34, 749
Sekiguchi, K., & Wolstencroft, R. D. 1993, MNRAS, 263, 349
Shi, F., Kong, C. Li, Cheng, F. Z. 2005, A&A, 437, 849
van den Broek, A. C., et al. 1991, A&AS, 91, 61
Veilleux, S., et al. 1995, ApJS, 98, 171
Waller, W. H. 1991, ApJ, 370, 144
Werner, M. W., et al. 2004, ApJS, 154, 1
Wu, H., Cao, C., & Hao, C-N. 2005, ApJ, 632, L79